Hemodynamic conditions in a failing peripheral artery bypass graft

Patrick M. McGah, MS,[a] Daniel F. Leotta, PhD,[b] Kirk W. Beach, PhD, MD,[c] R. Eugene Zierler, MD,[c] James J. Riley, PhD,[a] and **Alberto Aliseda, PhD,[a]** *Seattle, Wash*

Objective: **The mechanisms of restenosis in autogenous vein bypass grafts placed for peripheral artery disease are not completely understood. We investigated the role of hemodynamic stress in a case study of a revised bypass graft that failed due to restenosis.**

Methods: **The morphology of the lumen was reconstructed from a custom three-dimensional ultrasound system. Scans were taken at 1, 6, and 16 months after a patch angioplasty procedure. Computational hemodynamic simulations of the patient-specific model provided the blood flow features and the hemodynamic stresses on the vessel wall at the three times studied.**

Results: **The vessel was initially free of any detectable lesions, but a 60% diameter-reducing stenosis developed during the 16-month study interval. As determined from the simulations, chaotic and recirculating flow occurred downstream of the stenosis due to the sudden widening of the lumen at the patch location. Curvature and a sudden increase in the lumen cross-sectional area induced these flow features that are hypothesized to be conducive to intimal hyperplasia. Favorable agreement was found between simulation results and in vivo Doppler ultrasound velocity measurements.**

Conclusions: **Transitional and chaotic flow occurs at the site of the revision, inducing a complex pattern of wall shear as computed with the hemodynamic simulations. This supports the hypothesis that the hemodynamic stresses in the revised segment, produced by the coupling of vessel geometry and chaotic flow, led to the intimal hyperplasia and restenosis of the graft. (J Vasc Surg 2012;56:403-9.)**

The failure rate of autogenous vein bypass grafting for the treatment of peripheral artery disease remains high, at up to 20% within the first year of implantation and up to 50% within 5 years.[1-3] Graft failure usually follows development of stenotic lesions brought on by intimal hyperplasia. Up to 70% of lower extremity bypass grafts require reintervention to correct stenotic lesions.[4]

Autogenous venous grafts will adapt to the conditions of the arterial circulation in the first few months after surgery (ie, arterialization). The morphologic and structural changes that occur during the remodeling process include an increase in graft lumen cross-section[5,6] as well as medial and intimal thickening of the graft wall.[7,8] The adaptive remodeling of the graft is widely understood to be stimulated by hemodynamic forces.[9]

The remodeling in the intima can degenerate into an uncontrolled proliferation process (ie, intimal hyperplasia). Vascular medial smooth muscle cells and adventitial fibroblasts proliferate,[10] migrate into the intima, and deposit extracellular matrix, locally inducing a stenotic lesion that jeopardizes graft patency. Although the exact biologic mechanisms that trigger intimal hyperplasia remain unknown, hemodynamic wall shear stress has consistently been shown to influence the outcome of intimal thickening. A clinical study of morphologic changes in revised peripheral artery bypass grafts[11] showed a broad range of remodeling responses. Many of the grafts experienced significant lumen narrowing or stenoses after revision. However, most stenoses regressed, while some continued to progress and required clinical intervention. Animal models of vein arterialization, however, have shown that the extent of intimal hyperplasia in grafts is inversely proportional to the wall shear stress magnitude.[8,12-15]

Direct detailed measurements of in vivo hemodynamics remain challenging, even with recent advances in Doppler ultrasound and phase-contrast magnetic resonance imaging. Limitations in spatial and temporal resolution result in high uncertainty in the estimation of shear stress, particularly in regions of transitional or chaotic flow. Advances in computational fluid dynamics provide useful tools to quantify the complex flow features and shear stress patterns present in bypass grafts. Computational fluid simulations have been used to examine hemodynamic forces in idealized[16-20] and patient-specific geometries.[21-23] These simulations achieve a high level of temporal resolution (0.1 ms) and spatial resolution (0.1 mm) not attainable in in vivo or in vitro experiments.[24] This level of resolution is essential to understand the details of the interaction between blood flow and tissue remodeling. These studies have shown that some regions of low wall shear stress (<0.5 Pa), such as anastomoses, correlate with regions of intimal thickening as determined by histologic examinations.[25]

From the Department of Mechanical Engineering,[a] Center for Industrial and Medical Ultrasound,[b] and Department of Surgery, Division of Vascular Surgery,[c] University of Washington.

This work has been supported by an R21 grant from NIDDK (DK08-1823).

Author conflict of interest: none.

Reprint requests: Patrick M. McGah, Department of Mechanical Engineering, Stevens Way Box 352600, Seattle, WA 98195 (e-mail: pmcgah@u.washington.edu).

The editors and reviewers of this article have no relevant financial relationships to disclose per the JVS policy that requires reviewers to decline review of any manuscript for which they may have a conflict of interest.

0741-5214/$36.00

doi:10.1016/j.jvs.2012.01.045

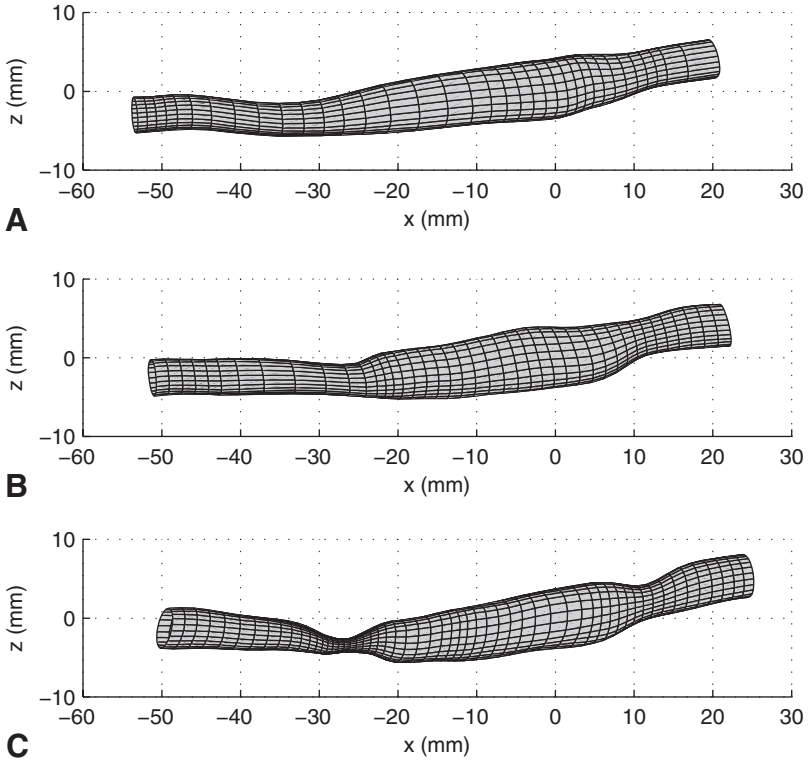

Fig 1. Surface reconstructions of the three bypass grafts registered in a common coordinate system. Reconstructions are chronologic from *top* to *bottom*. Times of acquisition are **(A)** 1 month, **(B)** 6 months, and **(C)** 16 months after a polytetrafluoroethylene patch angioplasty. The patch is approximately located between $x = -30$ mm to $x = +10$ mm and covers about one-third of the vessel circumference.

Despite the attention focused on this problem, no definitive link has been established between hemodynamic forces and long-term patency. There have been surprisingly few longitudinal in vivo studies of graft remodeling associated with detailed hemodynamic computations.[22,23] Unfortunately, many in vivo studies correlating shear stress to intimal hyperplasia[5,6,12,14,15] have used simplified relationships for computing wall shear stresses (ie, Poiseuille's law). Transitional or recirculating flows, or both, both critical in the development of intimal hyperplasia,[9] are not well described with such simplistic fluid mechanical theories.

We conducted a longitudinal retrospective case study of a revised autogenous arterial bypass graft for 16 months after a patch angioplasty. We previously reported the methodology followed here and the hemodynamics of this case,[24] and in this report, present new analyses and new conclusions with relevance to clinical practice. We combine hemodynamic computational simulations in the three patient-specific geometries reconstructed from three-dimensional (3D) ultrasound imaging at 1, 6, and 16 months after surgery. We correlate the observed in vivo evolution of the vessel wall remodeling with the computational wall shear stresses, with the goal of determining the role of mechanical stresses on the changes in the lumen.

METHODS

Patient history. A femoral to above-knee popliteal artery reversed saphenous vein graft was studied under a protocol approved by the University of Washington Human Subjects Division. Our study begins with a revision performed 7 years after initial graft placement, due to stenosis formation at a venous valve site. The revision consisted of an endarterectomy and polytetrafluoroethylene patch angioplasty. Postoperative ultrasound scans of the graft were performed at 1, 6, and 16 months after the revision procedure. At 20 months after the revision, the graft segment was replaced by an interposition graft due to restenosis accompanied by symptoms of increasing claudication.

Ultrasound imaging and 3D reconstruction. Ultrasound imaging was performed with a custom 3D system, as described previously.[26] Briefly, a magnetic tracking system (Flock of Birds; Ascension Technology, Burlington, Vt) provides the location and orientation of the ultrasound scan head during the examination. The ultrasound imager (HDI 5000; Philips Medical Systems, Bothell, Wash) and magnetic tracking system are interfaced with a personal computer using custom software for simultaneous acquisition of the ultrasound images and location data. Data acquisition is gated to an electrocardiograph (ECG) signal.

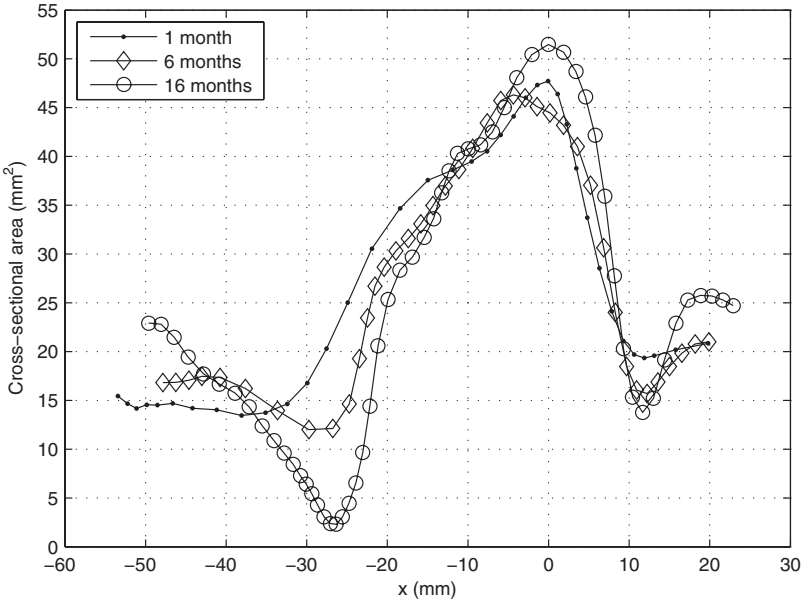

Fig 2. Cross-sectional area measurements vs graft axis for three surface reconstructions. Coordinate system is the same as that in Fig 1.

Cross-sectional images were obtained at intervals of 1 to 2 mm along the graft segment of interest. The ECG trigger was set to ensure that the data were gathered when velocity was maximal (200 ms after ECG systole). Doppler spectral waveforms were also recorded at 5- to 20-mm intervals along the length of the revised segment. All ultrasound measurements were performed with the patient supine. The cross-sectional images of the entire length of the graft took 6 to 7 minutes to acquire.

Custom MATLAB (The MathWorks, Natick, Mass) scripts are used to reconstruct 3D surfaces from the ultrasound images.[11,26] Automatic color segmentation defines the boundary of the lumen on each 2D cross-sectional power Doppler view of the vessel. The contours are transformed to locations in the 3D coordinate system by use of the position and orientation information associated with each image plane. Registration of data sets across visits is accomplished by correlation of cross-sectional area profiles computed from the reconstructed 3D surfaces.[11] The 3D surface reconstructions of the three scans registered in a common coordinate system are shown in Fig 1. The cross-sectional area measurements from those scans are shown in Fig 2.

Computational methods. The flow equations are solved with a Computational Fluid Dynamics software package (ANSYS FLUENT 12.1; ANSYS Inc, Cannonsburg, Pa), calculating the velocity and pressure on the points of a computational mesh created by GAMBIT (ANSYS). Well-accepted assumptions on blood rheology, rigid vessel wall conditions, and blood flow profile at the inlet were used in the simulation, as described in McGah et al.[24]

Errors in the measurement of the cross-sectional area of the vessel lumen were estimated to be within $\pm 14\%$,[11] whereas errors in the flow rate measurements are $\sim \pm 13\%$.[27] Previous analysis places the error of the simulation itself at $< \pm 6\%$.[24]

RESULTS

The entire graft underwent appreciable remodeling over the course of the three clinical visits. This remodeling was concentrated in two distinct regions. First, a stenosis developed at the proximal end of the patch. This can be seen in the cross-sectional area reduction at the $x = -30$-mm location in Figs 1 and 2. The second region of significant vessel wall remodeling is at the distal end of the patch where a poststenotic dilatation is observed at the $x = 0$ location in Figs 1 and 2.

A time-dependent velocity within the graft is obtained from the maximum velocity of the Doppler ultrasound spectral waveforms applied at the centerline velocity of the vessel.[28] This is converted to a flow rate and imposed as the condition driving the flow in the simulations. Flow rates are shown in Fig 3. The time-averaged flow rate was 130 mL/min, with a peak of 510 mL/min for the 1 and 6 month examinations. At 16 months, the time-averaged and maximum flow rates were 86.4 and 410 mL/min, respectively. These values corresponded to mean Reynolds numbers (the key nondimensional parameter that controls transition from laminar to turbulent flow) of 176 at 1 and 6 months and 110 at 16 months. The ECG-measured patient heart rate in beats/min was 56 to 61 at 1 month, 54 to 58 at 6 months, and 54 to 61 at 16 months. We used a representative value of 60 beats/min in all simulations.

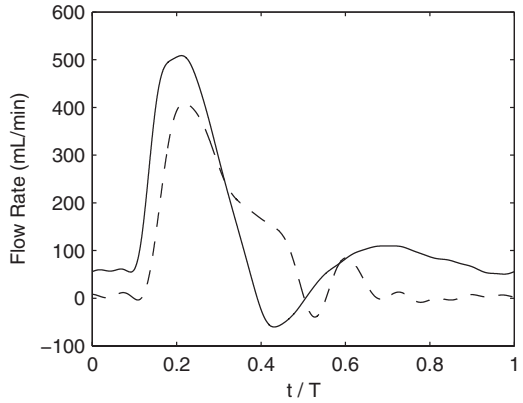

Fig 3. Volumetric flow rates applied at domain inlet (mL/min) vs time. The time has been normalized with the cardiac cycle period. The *solid line* is the flow rate used for 1 and 6 months, and the *dashed line* is the flow rate used at 16 months.

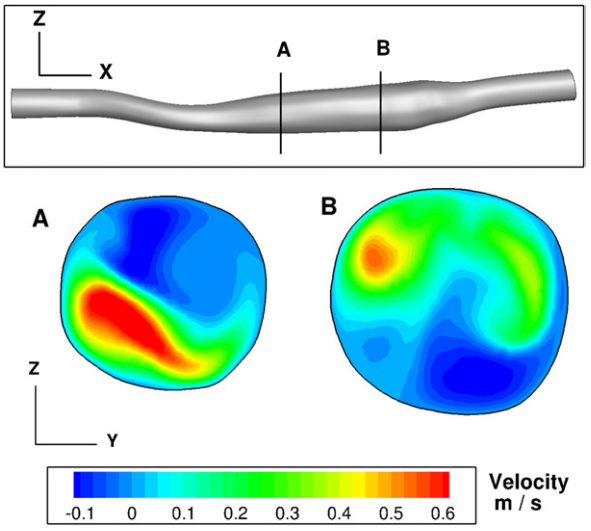

Fig 4. Simulated instantaneous stream-wise velocity contours of the 1-month scan at systolic deceleration (t/T = 0.3). Subfigures **A** and **B** depict the out-of-plane velocity at two planes located at $x = -27$ mm and -5 mm, respectively.

First, we examined the detached flow in light of the hypothesized connection of low shear stress to intimal hyperplasia. Second, we examined high-frequency chaotic flow fluctuations as a cause of the poststenotic dilatation.

Stenotic region. The proximal end of the patch changed from no stenosis at 1 month, to 15% diameter (25% area) reduction at 6 months, and to 60% diameter (85% area) reduction at 16 months after revision. Proximal to the patch anastomosis, the simulated flow was laminar for all cases. The simulated time-averaged wall shear stresses at the inflow segment of the revision are 1.61, 1.82, and 1.02 Pa at 1, 6, and 16 months, respectively, which is in agreement with previously published results of normal

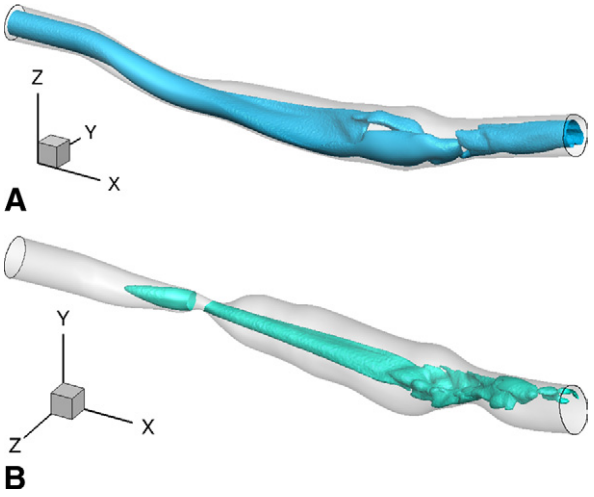

Fig 5. A, Surface of constant velocity at 1 month during midsystolic deceleration (t/T = 0.3). Value of velocity surface is 0.25 m/s. The velocity surface is smooth on the *left-hand side* of the figure but becomes less regular on the *right-hand side* due to the passage of flow vortices. **B,** Surface of constant velocity in the poststenotic jet at 16 months during midsystolic deceleration (t/T = 0.3). Value of velocity surface is 0.50 m/s. The shape of the velocity surface is irregular on the *right-hand side* of the figure, indicating the flow transition. Note that the value of the velocity surface in *B* is twice that of *A*. Flow is from *left* to *right* in both cases.

shear stress in femoral bypass grafts.[6] Flow separation occurs in the simulations distal to the start of the patch due to a sudden increase in the cross-sectional area of the lumen at $x = -30$ mm. Fig 4 shows the simulated velocity at two cross-sectional planes downstream from the location of the minimum cross-section. We observe flow recirculation (blue region on the top right side of Fig 4, *A*) and flow instability: the flow rolls into a pair of vortices that can be seen as a "crescent moon" filling the top half of the vessel (Fig 4, *B*). This alternating pattern of high-speed flow in part of the vessel cross-section and low or retrograde flow in the rest of the lumen, associated with the chaotic nature of this flow, leads to large spatiotemporal fluctuations of shear stress.

Doppler ultrasound velocimetry was performed at multiple locations along the graft. The 3D tracker was not activated during the collection of Doppler spectral waveforms (which were captured as part of the patient's standard clinical examination), so the exact location at which the Doppler spectra were taken cannot be quantitatively determined. However, this location can be estimated by examining the B-mode images that accompany each Doppler waveform. This allows us to compare the Doppler measurements from 1 and 6 months with the velocity measurements from the simulations at the same location. We observe spectral broadening, indicative of transitional/chaotic flow,[11] in the in vivo measurements (data not shown). This observation is consistent with the simulation results: flow separation, jet formation, and recirculating

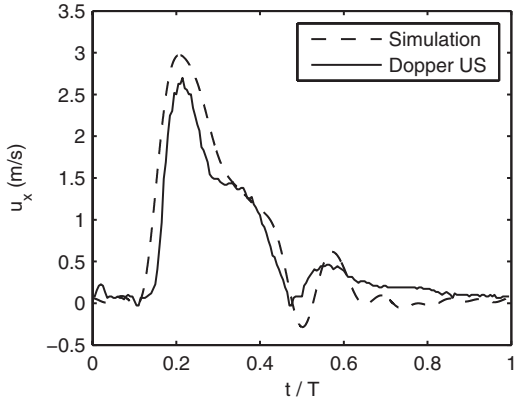

Fig 6. Simulated (*dashed line*) and Doppler ultrasound (*US*; *solid line*) documented in vivo velocity vs time at the center of the stenosis for one cardiac cycle (examination at 16 months).

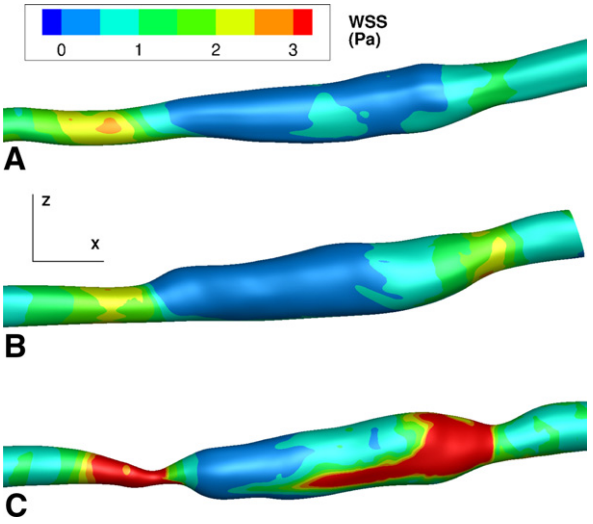

Fig 7. Time-averaged wall shear stress (*WSS*) contours on the graft lumen (in Pa). Images are **(A)** 1 month, **(B)** 6 months, and **(C)** 16 months. Flow is from *left* to *right*. Shear patterns are approximately symmetric on the reverse side of the lumen.

vortical flow (as seen in Fig 4). Fig 5, *A* shows a 3D visualization of the flow transition in the patched segment for the visit at 1 month.

At 16 months, the hemodynamics in the graft were markedly different from the first visits. Doppler ultrasound at 16 months recorded peak systolic velocities of approximately 0.54 m/s proximal to the stenosis ($x = -45$ mm, not shown) with no signs of transitional flow. At the throat of the stenosis ($x = -27$ mm), peak systolic velocities were between 2.35 and 2.71 m/s. The simulation computed peak systolic velocities at this location were approximately 2.97 m/s (Fig 6 for a comparison between the in vivo and in silico stenosis velocities). This produces a poststenotic jet that persists throughout systole (Fig 5, *B*). The shear stress values computed at the stenosis throat (Fig 7, *bottom*

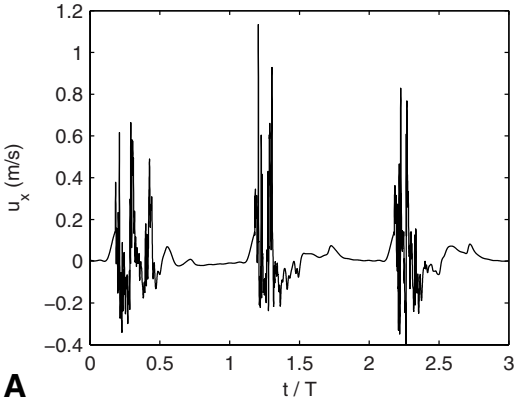

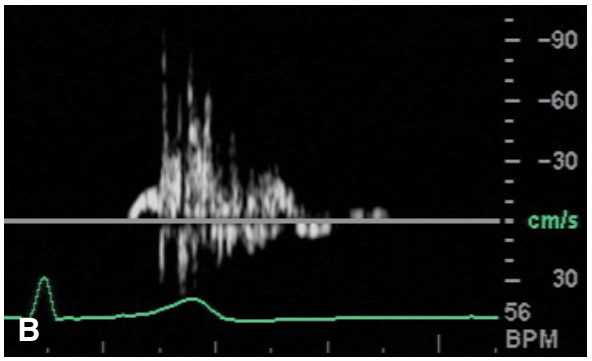

Fig 8. Simulated vs in vivo velocimetry for the visit at 16 months. **A,** Simulated stream-wise velocity vs time for three cardiac cycles at a point located at x = 0 in the center of the lumen. **B,** In vivo Doppler ultrasound velocimetry near the distal patch anastomosis for one cardiac cycle. Abscissa is the time (approximately 1 second) and the ordinate is the velocity (cm/s).

panel) are much greater than predicted by Poiseuille's law. The time-averaged wall shear stress is >30 Pa in this section of the graft, and the instantaneous wall shear stress is >100 Pa during peak systole. This is a pathologic level of shear stress and is expected to strongly influence endothelial function, considering that the peak systolic shear stresses computed at the stenotic segment is 6.33 Pa at 1 month and 7.05 Pa at 6 months. The three panels in Fig 7 display a rendering of the time-averaged shear stress acting on the vessel lumen at the three visits, allowing us to observe the spatial and temporal patterns of wall shear stress as the vessel remodels.

Poststenotic dilatation. The poststenotic jet becomes unstable and transitions into a chaotic state, particularly during systolic deceleration (the Reynolds number for the jet, based on the stenosis diameter and the peak velocity, is ~1500 at the 16-month scan). Fig 5, *B* shows a 3D surface of constant velocity where the poststenotic jet is observed to impinge on the graft wall several centimeters distal to the stenosis. The vortices impinging on the graft wall produce very high shear stresses and high frequency pressure fluctuations on the vessel wall.

The in vivo Doppler measurements made in the poststenotic region at 16 months also show spectral broadening and reversed flow during systole (Fig 8, *A*), indicative of flow transition/turbulence in the fluid jet. For comparison, computed flow waveforms in the poststenotic region also show high frequency fluctuations during systole and relatively quiescent motion during diastole (Fig 8, *B*).

DISCUSSION

Our simulations show that transitional or chaotic flow can easily occur in arterial conduits despite the flow conditions being well below the classic value of 2000 for the Reynolds number for laminar-to-turbulent transition in steady pipe flow.[29] The two primary reasons for the early transition from laminar flow in this study are (1) rapidly changing lumen cross-section and (2) flow pulsatility. In the patched region, the lumen cross-section expands by nearly a factor of three. The flow must slow down approximately by a factor of three to satisfy conservation of mass, giving rise to an adverse pressure gradient due to the Venturi effect (whereby the flow pressure downstream increases as the flow decelerates). The adverse pressure gradient "pushes back" onto the fluid near the vessel wall as it decelerates through the expansion. If the inertia of the fluid is not strong enough, the fluid can no longer move forward in a streamlined fashion and separation occurs.[29] The flow deceleration after peak systole enhances the adverse pressure gradient and therefore the incidence of separation. A third factor that alters the threshold for laminar transition is the curvature of the blood vessel. Vessel curvature can also enhance adverse pressure gradients and induce secondary flows.

The altered hemodynamics occurring in the region of flow separation creates localized low wall shear stress (<0.5 Pa), which is particularly pronounced at the proximal region of the patch at 1 month after revision. In subsequent scans, a significant stenosis develops at a location coincident with a localized flow transition. This is in agreement with the widespread hypothesis[9] that there is a feedback loop, whereby localized flow instabilities induce altered hemodynamic stresses (such as low shear stress <0.5 Pa) and subsequently lead to endothelial dysfunction, misregulation of smooth muscle cells and fibroblasts, and ultimately, intimal hyperplasia. This, in turn, might enhance the development of stenosis that feeds back into the flow instability.[10,14,15]

Furthermore, we propose that there exists an optimal graft diameter after patch angioplasty that would maximize the likelihood of long-term patency. The graft diameter should be large enough to ensure sufficient blood flow to the distal tissue but not so large that flow separation and recirculation occur, which could accelerate intimal hyperplasia. Specification of the optimal diameter for a given patient-specific configuration is a topic for further study.

Certainly, additional factors beyond hemodynamics are related to the generation of stenoses. We hypothesize that physiologic factors, such as a localized loss of endothelial function, pre-existing venous lesions, or denudation due to surgical injury, are coadjuvant to the effect of low shear on intimal hyperplasia. Furthermore, it has long been speculated that the injury sustained during the surgery or the repeated stretching of the graft due to the compliance mismatch between the autogenous graft and the polytetrafluoroethylene induces a proliferative cellular response in the intima.[13] However, it has also long been speculated that the endothelium mitigates the proliferative response when subjected to normal values of wall shear stress by releasing nitric oxide or prostacyclin.[9,12] Therefore, we conjecture that altered hemodynamic forces are likely one of many confluent factors influencing vein graft patency. The focal nature of vein graft stenosis may be explained by the colocalization of vessel injury and nonlaminar flow shear stresses.

We found a poststenotic dilatation in the graft region distal to the stenosis. We hypothesize that the jet formed at the stenosis transitions to turbulence and impinges on the graft wall, inducing high frequency fluctuations in the mechanical stresses that elicit the dilatory response. Our simulations do not calculate wall stretch, but the high frequency flow fluctuations would induce bruits corresponding to the frequencies of flow fluctuations (50-200 Hz). We speculate that mechanical stretch due to pressure fluctuations as well as flow shear stress, which is assumed to reduce muscular tone via nitric oxide,[9] initiate a response in endothelial cells that stimulates the vessel dilation. However, future studies are needed to differentiate the role of stretch vs shear in poststenotic dilatation.

We acknowledge several limitations to this study. First, histologic analysis of the failed vein graft segment was not conducted because it was eventually bypassed by an interposition graft and not excised. Because it is impossible to know the distribution and extent of intimal hyperplasia within the graft, a quantitative correlation between low shear and intimal thickness cannot be made.

Second, this case study involves only one patient. We can show an association between transitional flow and remodeling, but we cannot prove causality. Further case-control studies will be needed to validate this hypothesis.

Third, more frequent monitoring of grafts in conjunction with hemodynamic simulations, for example at 1-month intervals during the first 3 months after surgery, when the wall remodeling occurs at its fastest rate,[6,11] are necessary to further elucidate the feedback process between changes in flow and lumen cross-section.

CONCLUSIONS

This study presents the application of ultrasound image-based computational modeling to the study of peripheral artery graft remodeling and failure. Simulations in a failing peripheral artery bypass graft allow us to quantify the hemodynamic stresses and to illustrate the interplay between flow and remodeling and can serve as a complement to standard in vivo ultrasound surveillance. The availability, ease of use, and temporal resolution of ultrasound provide it with certain advantages over other imaging modalities for biomechanics simulations. Computational simulations,

coupled with longitudinal patient scans, have the potential to reveal complex hemodynamic features, their role in determining long-term morphologic changes, and more important, clinical outcomes.

AUTHOR CONTRIBUTIONS

Conception and design: PM, DL, KB, AA
Analysis and interpretation: PM, DL, KB, RZ, JR, AA
Data collection: PM, DL
Writing the article: PM, AA
Critical revision of the article: PM, DL, KB, JR, RZ, AA
Final approval of the article: PM, DL, KB, JR, RZ, AA
Statistical analysis: PM, DL, KB, AA
Obtained funding: DL, AA
Overall responsibility: PM

REFERENCES

1. Goodney PP, Beck AW, Nagle J, Welch HG, Zwolak RM. National trends in lower extremity bypass surgery, endovascular interventions, and major amputations. J Vasc Surg 2009;50:54-60.
2. Mills JL, Bandyk DF, Gahtan V, Esses GE. The origin of infrainguinal vein graft stenoses: a prospective study based on duplex surveillance. J Vasc Surg 1995;21:16-25.
3. Watson HR, Buth J, Schroeder TV, Simms MH, Horrocks M. Incidence of stenoses in femorodistal bypass vein grafts in a mulicentre study. Eur J Vasc Endovasc Surg 2000;20:67-71.
4. Conte MS, Bandyk DF, Clowes AW, Moneta GL, Seely L, Lorenz TJ, et al. Results of PREVENT III: a multicenter, randomized trial of edifolidge for the prevention of vein graft failure in lower extremity bypass surgery. J Vasc Surg 2006;43:742-51.
5. Fillinger MF, Cronenwett JL, Besso S, Walsh DB, Zwolak RM. Vein adaptation to the hemodynamic environment of infrainguinal grafts. J Vasc Surg 1994;19:970-8.
6. Owens CD, Wake N, Jacot JG, Gerhard-Herman M, Gaccione P, Belkin M, et al. Early biomechanical changes in lower extremity vein grafts--distinct temporal phases of remodeling and wall stiffness. J Vasc Surg 2006;44:740-6.
7. Dobrin PB. Mechanical factors associated with the development of intimal and medial thickening in vein grafts subjected to arterial pressure. A model of arteries exposed to hypertension. Hypertension 1995; 26:38-43.
8. Galt SW, Zwolak RM, Wagner RJ, Gillbertson JJ. Differential response of arteries and vein grafts to blood flow reduction. J Vasc Surg 1993; 17:563-70.
9. Owens CD. Adaptive changes in autogenous vein grafts for arterial reconstruction: clinical implications. J Vasc Surg 2010;51:736-46.
10. Kalra M, Miller VM. Early remodeling of saphenous vein grafts: proliferation, migration and apoptosis of adventitial and medial cells occur simultaneously with changes in graft diameter and blood flow. J Vasc Res 2000;37:576-84.
11. Leotta DF, Primozich JF, Beach KW, Bergelin RO, Zierler RE, Strandness DE Jr. Remodeling in peripheral vein graft revisions: serial study with three-dimensional ultrasound imaging. J Vasc Surg 2003;37:798-807.
12. Kohler TR, Kirkman TR, Kraiss LW, Zierler BK, Clowes AW. Increased blood flow inhibits neointimal hyperplasia in endothelialized vascular grafts. Circ Res 1991;69:1557-65.
13. Bassiouny HS, White S, Glagov S, Choi E, Giddens DP, Zarins CK. Anastomotic intimal hyperplasia: mechanical injury or flow induced. J Vasc Surg 1992;15:708-17.
14. Meyerson SL, Skelly CL, Curi MA, Shakur UM, Vosicky JE, Glagov S, et al. The effects of extremely low shear stress on cellular proliferation and neointimal thickening in the failing bypass graft. J Vasc Surg 2001;34:90-7.
15. Jiang Z, Wu L, Miller BL, Goldman DR, Fernandez CM, Abouhamze ZS, et al. A novel vein graft model: adaption to differential flow environments. Am J Physiol Heart Circ Physiol 2003;286:240-5.
16. Lei M, Archie JP, Kleinstreuer C. Computational design of a bypass graft that minimizes wall shear stress gradients in the region of the distal anastomosis. J Vasc Surg 1997;25:637-46.
17. Lei M, Giddens DP, Jones SA, Loth F, Bassiouny HS. Pulsatile flow in and end-to-side vascular graft model: comparison of computations with experimental data. J Biomech Engr 2001;123:80-7.
18. Walsh MT, Kavanagh EG, O'Brien T, Grace PA, McGloughlin T. On the existence of an optimum end-to-side junctional geometry in peripheral bypass surgery--a computer generated study. Eur J Vasc Endovasc Surg 2003;26:649-56.
19. O'Brien TP, Grace P, Walsh M, Burke P, McGloughlin T. Computational investigations of a new prosthetic femoral-popliteal bypass graft design. J Vasc Surg 2005;42:1169-75.
20. Pousset Y, Lermusiaux P, Berton G, Le Gouez JL, Leroy R. Numerical model study of flow dynamics through an end-to-side anastomosis: choice of anastomosis angle and prosthesis diameter. Ann Vasc Surg 2006;20:773-9.
21. Moore JA, Steinman DA, Prakash S, Johnston KW, Ethier CR. A numerical study of blood flow patterns in anatomically realistic and simplified end-to-side anastomoses. J Biomech Engr 1999;121:265-72.
22. Giordana S, Sherwin SJ, Peiró J, Doorly DJ, Crane JS, Lee KE, et al. Local and global geometric influence on steady flow in distal anastomoses of peripheral bypass grafts. J Biomech Engr 2005;127:1087-98.
23. Jackson M, Wood NB, Zhao S, Augst A, Wolfe JH, Gedroyc WM, et al. Low wall shear stress predicts subsequent development of wall hypertrophy in lower limb bypass grafts. Artery Res 2009;3:32-8.
24. McGah PM, Leotta DF, Beach KW, Riley JJ, Aliseda A. A longitudinal study of remodeling in a revised peripheral artery bypass graft using 3D ultrasound and computational hemodynamics. J Biomech Eng 2011; 133:041008.
25. Loth F, Fischer PF, Bassiouny HS. Blood flow in end-to-side anastomoses. Annu Rev Fluid Mech 2008;40:367-93.
26. Leotta DF, Primozich JF, Beach KW, Bergelin RO, Strandness DE Jr. Serial measurement of cross-sectional area in peripheral vein grafts using three-dimensional ultrasound. Ultrasound Med Biol 2001;27:61-8.
27. Zierler BK, Kirkman TR, Kraiss LW, Reiss WG, Horn JR, Bauer LA, et al. Accuracy of duplex scanning for measurement of arterial volume flow. J Vasc Surg 1992;16:520-6.
28. Womersley JR. Method for the calculation of velocity, rate of flow and viscous drag in arteries when the pressure gradient is known. J Physiol 1955;127:553-63.
29. Kundu PK, Cohen IM. Fluid mechanics. 3rd ed. San Diego; Elsevier Academic Press; 2000.

Submitted Sep 20, 2011; accepted Jan 14, 2012.